

Super-Resolution of Brain MR Images based on Sparse Representations

Andrea Rueda^a, Eduardo Romero^{a,*}

^a*BioIngenium Research Group, Universidad Nacional de Colombia, Bogotá, Colombia.*

Abstract

The problem of Partial Volume (PV) in Magnetic Resonance (MR) images is due to the limited spatial resolution of the MR equipment, causing blurring at the interfaces between tissues. Together with noise and intensity inhomogeneities, the PV effect affects the precision of the tissue segmentation task, producing misclassification of voxels and distorting quantitative results of posterior morphometry tasks such as cortical thickness estimation. This paper presents the application of a already-proposed methodology for super-resolution of images, based on sparse representations, that attempts to overcome the PV effect by generating a high-resolution version of a brain MR image.

Keywords: Partial volume effect, image super-resolution, sparse representations

1. Introduction

In magnetic resonance imaging (MRI), the accuracy and precision with which brain structures may be quantified is frequently affected by the partial volume (PV) effect. PV is due to the limited spatial resolution of MRI compared to the size of anatomical structures, as shown in Figure 1. Accurate classification of mixed voxels and correct estimation of the proportion of each pure tissue (fractional content) may help to increase the precision of cortical thickness in regions where the measure is particularly difficult such as deep sulci. Two issues arise when it comes to classification of mixed voxels and accurate computation of fractional content. Firstly, in deep sulci regions, where two banks of the cortex are in contact, mixed tissue voxels

*Corresponding Author: Eduardo Romero. Carrera 30 45-03, Ed. 471 School of Medicine, +57 1 3165491, edromero@unal.edu.co

may be mislabelled as another tissue type. Secondly, intensity and contrast of the pure tissue types can spatially vary, because of the nature of the cytoarchitecture and may bias the accurate estimation of the fractional content, even after correction of intensity inhomogeneity.

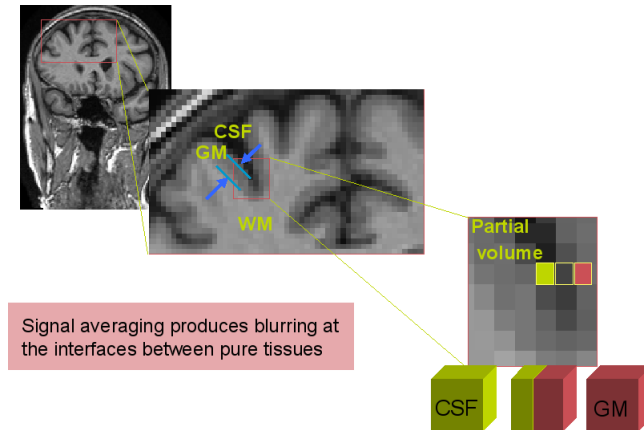


Figure 1: Illustration of partial volume (PV) effect

2. Super-Resolution of Images

One of the most classical inverse problems in image processing is the so-called super resolution or image magnification problem. The idea is to generate a high-resolution version of a given low-resolution image, where the sharpness and naturalness match those of true high-resolution images.

Given a low-resolution image $Y \in \mathbb{R}^q$, the objective is to recover a higher-resolution image $X \in \mathbb{R}^n$ of the same scene (where $q < n$). The relation between the two images can be modeled as (reconstruction constraint)

$$Y = \mathbf{S}\mathbf{H}X = \mathbf{L}X \quad (1)$$

where \mathbf{H} is a linear (blurring) filter, \mathbf{S} is a down-sampling operator and $\mathbf{L} = \mathbf{S}\mathbf{H}$. This means that the observed low-resolution image Y is a blurred and downsampled version of the solution X .

The sparse representation of the high-resolution image cannot be directly computed, because proper regularization is needed to obtain a unique and “good” solution. Instead, we will work on small patches x of X , with two coupled dictionaries: \mathbf{D}_h for high-resolution patches and $\mathbf{D}_l = \mathbf{L}\mathbf{D}_h$ for low-resolution patches. The sparse representation of a low-resolution

patch in terms of \mathbf{D}_l will be directly used to recover the corresponding high-resolution patch from \mathbf{D}_h . The patches x of the high-resolution image X can be represented as

$$x = \mathbf{D}_h \alpha \quad (2)$$

for some $\alpha \in \mathbb{R}^k$ with $\|\alpha\|_0 \leq k$. Thus, the super resolution problem becomes that of recovering α from low-dimensional measurements

$$y = \mathbf{L}x = \mathbf{L}\mathbf{D}_h \alpha \quad (3)$$

Thus, we may attempt to recover α by solving $\mathcal{P}_p(\mathbf{D}_l, y, \delta)$ or $\mathcal{G}_p(\mathbf{D}_l, y, \lambda)$. In practice, the problem could be divided into two steps, as presented in [1]. First, a sparse representation for each local patch is found using the sparse prior (2), respecting spatial compatibility between neighbors. Then, using this result, the entire image is further regularized and refined using the reconstruction constraint (1). This strategy then uses a local model from the sparse prior to recover lost high-frequencies for local details, while a global model from the reconstruction constraint is further applied to remove possible artifacts and assure consistency and naturalness of the final result.

2.1. Local Model from Sparse Representation

For each input low-resolution patch y , the idea is to find a sparse representation in terms of the low-resolution dictionary patches \mathbf{D}_l . Then, the corresponding high-resolution patches in the dictionary \mathbf{D}_h will be combined according to these coefficients to generate the high-resolution reconstructed patch x . The problem can be formulated as

$$\min \|\alpha\|_0 \quad \text{s.t.} \quad \|F\mathbf{D}_l \alpha - Fy\|_2^2 \leq \epsilon \quad (4)$$

or, in an equivalent formulation using Lagrange multipliers

$$\min \lambda \|\alpha\|_1 + \frac{1}{2} \|F\mathbf{D}_l \alpha - Fy\|_2^2 \quad (5)$$

where the parameter λ balances sparsity of the solution and fidelity of the approximation to y . The introduction of F , a linear feature extraction operator, is needed to ensure that the computed coefficients fit the most relevant part of the low-resolution signal.

To enforce compatibility between adjacent patches we use a one-pass algorithm, where the patches are processed in raster-scan order (from left to right and top to bottom) with an overlapping between each patch and its previous neighbors. To include the information in the overlap, that constrain the super-resolution reconstruction of patch y to closely agree with

the previously computed adjacent high-resolution patches, the optimization problem can be reformulated as

$$\min \lambda \|\alpha\|_1 + \frac{1}{2} \|\tilde{\mathbf{D}}\alpha - \tilde{y}\|_2^2 \quad (6)$$

where $\tilde{\mathbf{D}} = \begin{bmatrix} F\mathbf{D}_l \\ \beta P\mathbf{D}_h \end{bmatrix}$ and $\tilde{y} = \begin{bmatrix} Fy \\ \beta w \end{bmatrix}$. Here, the matrix P extract the region of overlap between current patch and previously reconstructed high-resolution image for each patch in the dictionary, and w contains the values on the overlap of the already reconstructed high-resolution image. Finally, the parameter β controls the tradeoff between the low-resolution and the high-resolution information available for solving the problem.

2.2. Global Reconstruction Constraint

Because that the local model do not demand exact equality between the low-resolution patch and its reconstruction in terms of the dictionary \mathbf{D}_l , and also because of noise, the high-resolution image produced with the sparse representation may not satisfy the reconstruction constraint (1) exactly. To minimize the reconstruction error, a new optimization problem can be formulated as

$$X^* = \arg \min_X \|X - X_0\| \quad \text{s.t. } \mathbf{S}\mathbf{H}X = Y \quad (7)$$

To compute efficiently the solution to this problem, a backprojection (iterative gradient-based minimization) method is applied iteratively to the complete reconstructed high-resolution image:

$$X_{t+1} = X_t + ((Y - \mathbf{S}\mathbf{H}X_t) \uparrow s) * p \quad (8)$$

where X_t is the estimate of the high-resolution image at the t -th iteration, p is a backprojection filter, and $\uparrow s$ denotes upsampling by a factor of s .

2.3. Image Super-Resolution Algorithm

The complete super-resolution process is summarized in the Algorithm 1.

3. Experiments

The whole implementation of the image super-resolution algorithm has been done in MATLAB R14, with the SparseLab¹ library that provides a

¹<http://sparselab.stanford.edu/>

Algorithm 1 Image Super-Resolution via Sparse Representations

Require: training dictionaries \mathbf{D}_h and \mathbf{D}_l , a low resolution image Y
 for each patch y of Y , taken starting from the upper-left corner with an overlap in each direction **do**
 Solve the optimization problem (find α^* through Equation 6) with \tilde{D} and \tilde{y} as defined previously
 Generate the high-resolution patch with $x = \mathbf{D}_h \alpha^*$
 Put the patch x into the high-resolution image X_0
 end for
 Solve the optimization problem (Equation 7) using backprojection (Equation 8), to find the closest image to X_0 which satisfies the reconstruction constraint (1)
 return the super-resolution image X^*

set of solvers for the optimization problem (from this library we have chosen the Basis Pursuit solver). For all experiments, the λ parameter was set to $50 \times \dim(\text{patch feature})$, and the β parameter was set to 1.

3.1. Experiment 1: Reconstruction from a single image

We start with a single high-resolution training image X (grayscale, 630×519 pixels) and its corresponding low-resolution image Y (grayscale, 210×173 pixels), obtained by blurring and downsampling (in 1/3) the image X , as shown in Figure 2. In this experiment, we select the magnification factor as 3 (accordingly with the initial downsampling of the image). We extract 3×3 low-resolution patches, that corresponds to 9×9 high-resolution patches. The overlap between adjacent patches is set to 1 pixel in low-resolution, while in the high-resolution image this corresponds to an overlap of 3 pixels.

The coupled dictionaries \mathbf{D}_h and \mathbf{D}_l are constructed only from the low- and high-resolution versions of the image. We sample different quantities of patches (from 150 to 2100 patches) to test the influence of the dictionary size in the final result. Also, to observe the contribution of the local model and the backprojection step, we visualize the resulting image after each step. Figure 3 shows the results using an initial dictionary with 150 patches, while Figure 4 presents the results obtained using a dictionary with 2100 patches. As can be noticed, a large quantity of dictionary patches increases the level of detail in the reconstructed image. However, this also increases the computational cost of the procedure.

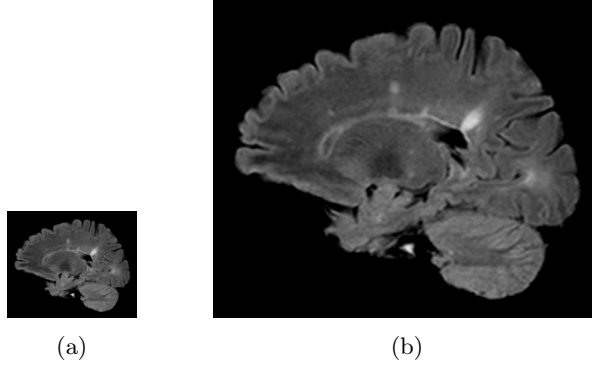


Figure 2: Training image: (a) Low-resolution version (210×173 pixels) (b) High-resolution version (630×519 pixels)

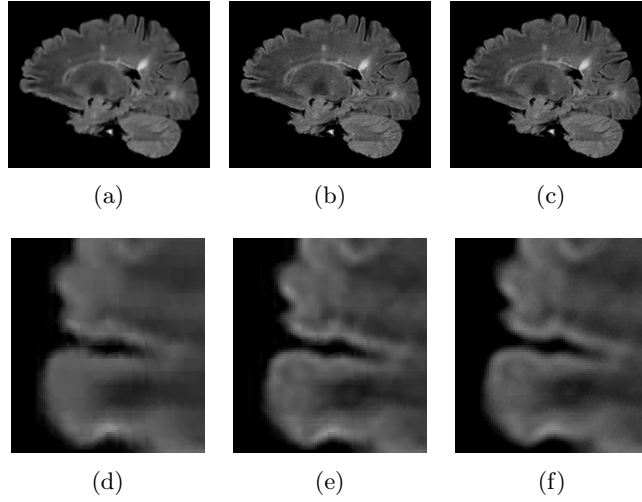


Figure 3: Reconstruction with 150 dictionary patches from a single image. (a), (d) High-resolution reconstruction after local model (b), (e) Final high-resolution reconstruction (c), (f) Original high-resolution image.

4. Conclusion

The preliminar results obtained by applying the image super-resolution method proposed by Yang et al [1] to MR images of the brain seems to be promising for eliminate the partial volume effects that affects the tissue segmentation and further morphometrical tasks. Further work includes to study the inclusion of spatial relationships on the segmented cortical sheet, in order to refine the high-resolution reconstruction particularly in the brain

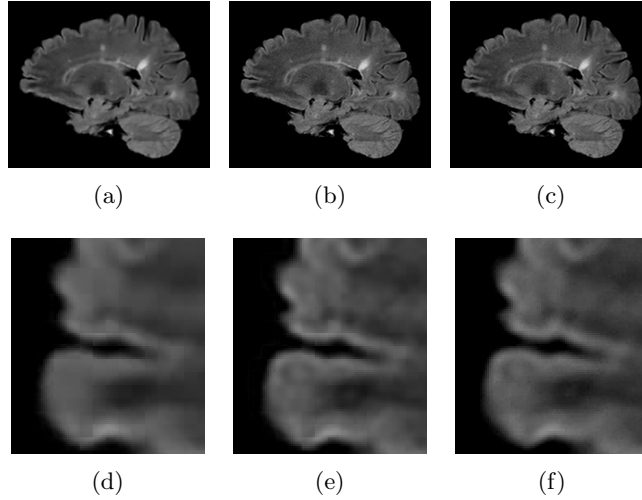


Figure 4: Reconstruction with 2100 dictionary patches from a single image. (a), (d) High-resolution reconstruction after local model (b), (e) Final high-resolution reconstruction (c), (f) Original high-resolution image.

folds and convolutions.

References

- [1] J. Yang, J. Wright, Y. Ma, T. Huang, Image super-resolution as sparse representation of raw image patches, in: Proceedings of the IEEE Conference on Computer Vision and Pattern Recognition, 2008, pp. 1–8.